Article

Cell

Decoding Neural Circuits that Control Compulsive Sucrose Seeking

Graphical Abstract

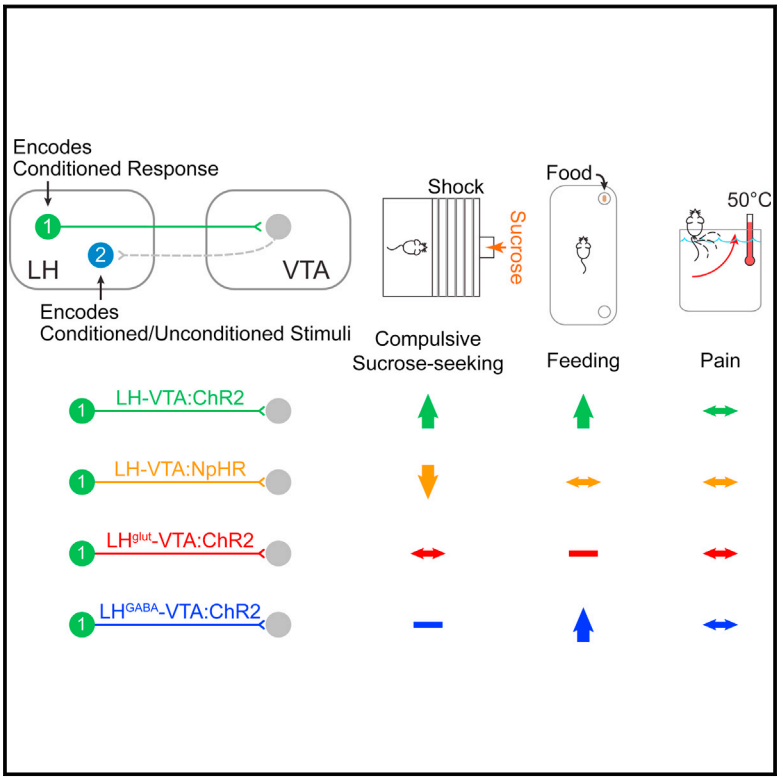

Authors

Edward H. Nieh, Gillian A. Matthews, ..., Craig P. Wildes, Kay M. Tye

Correspondence

kaytye@mit.edu

In Brief

A neural circuit loop between the lateral hypothalamus and the ventral tegmental area that selectively controls compulsive sugar consumption without preventing feeding necessary for survival provides a potential target for compulsive-overeating therapeutic interventions.

Highlights

- LH-VTA neurons encode reward-seeking actions after they transition to habits
- A subset of LH neurons downstream of VTA encode reward expectation
- LH-VTA projections provide bidirectional control over compulsive sucrose seeking
- Activating LH-VTA GABAergic projections increases maladaptive gnawing behavior

Nieh et al., 2015, Cell *160*, 528–541
January 29, 2015
http://dx.doi.org/10.1016/j.cell.2015.01.003

CellPress

Cell

Article

Decoding Neural Circuits that Control Compulsive Sucrose Seeking

Edward H. Nieh,[1,2] Gillian A. Matthews,[1,2] Stephen A. Allsop,[1,2] Kara N. Presbrey,[1] Christopher A. Leppla,[1] Romy Wichmann,[1] Rachael Neve,[1] Craig P. Wildes,[1] and Kay M. Tye[1,*]

[1]The Picower Institute for Learning and Memory, Department of Brain and Cognitive Sciences, Massachusetts Institute of Technology, Cambridge, MA 02139, USA

[2]Co-first author

*Correspondence: kaytye@mit.edu

http://dx.doi.org/10.1016/j.cell.2015.01.003

SUMMARY

The lateral hypothalamic (LH) projection to the ventral tegmental area (VTA) has been linked to reward processing, but the computations within the LH-VTA loop that give rise to specific aspects of behavior have been difficult to isolate. We show that LH-VTA neurons encode the learned action of seeking a reward, independent of reward availability. In contrast, LH neurons downstream of VTA encode reward-predictive cues and unexpected reward omission. We show that inhibiting the LH-VTA pathway reduces "compulsive" sucrose seeking but not food consumption in hungry mice. We reveal that the LH sends excitatory and inhibitory input onto VTA dopamine (DA) and GABA neurons, and that the GABAergic projection drives feeding-related behavior. Our study overlays information about the type, function, and connectivity of LH neurons and identifies a neural circuit that selectively controls compulsive sugar consumption, without preventing feeding necessary for survival, providing a potential target for therapeutic interventions for compulsive-overeating disorder.

INTRODUCTION

Tremendous heterogeneity exists across lateral hypothalamic (LH) neurons in terms of function and connectivity, and this can be observed by the variety of behaviors related to reward, motivation, and feeding linked with this region. However, little is known about how the LH computes specific aspects of reward processing and how this information is relayed to downstream targets. Electrical stimulation of the LH produces intracranial self-stimulation (ICSS) (Olds and Milner, 1954), as well as grooming, sexual, and gnawing behaviors (Singh et al., 1996). LH neurons encode sensory stimuli (Norgren, 1970; Yamamoto et al., 1989), including reward-associated cues (Nakamura et al., 1987). LH neurons also fire during both feeding (Burton et al., 1976; Schwartzbaum, 1988) and drinking (Tabuchi et al., 2002). However, making sense of the remarkable functional heterogeneity observed in the LH has been a major challenge in the field.

Although the LH is interconnected with many subcortical regions, we have a poor understanding of how the functional and cellular heterogeneity of the LH is transposed upon these anatomical connections. One LH projection target of interest is the ventral tegmental area (VTA), a critical component in reward processing (Wise, 2004). The LH-VTA projection was explored in early studies that used electrophysiological recordings combined with antidromic stimulation (Bielajew and Shizgal, 1986; Gratton and Wise, 1988). It has since been confirmed, using a rabies-virus-mediated tracing approach, that there is monosynaptic input from LH neurons onto dopamine (DA) neurons in the VTA (Watabe-Uchida et al., 2012). The VTA also sends reciprocal projections back to the LH, both directly and indirectly via other regions such as the nucleus accumbens, amygdala, hippocampus, and ventral pallidum (Barone et al., 1981; Beckstead et al., 1979; Simon et al., 1979).

Although both electrical (Bielajew and Shizgal, 1986) and optical (Kempadoo et al., 2013) stimulation have established a causal role for the LH projection to the VTA in ICSS, several questions remain to be answered. First, what is the neural response of LH-VTA neurons to different aspects of reward-related behaviors? Second, what is the role of the LH-VTA projection in reward seeking under different reinforcement contingencies? Third, what is the overall composition of fast transmission mediated by LH inputs to the VTA, and which VTA cells receive excitatory/inhibitory input? Finally, what do the excitatory and inhibitory components of the LH-VTA pathway each contribute toward orchestrating the pursuit of appetitive reward?

To address these questions, we recorded from LH neurons in freely moving mice and used optogenetic-mediated photoidentification to overlay information about the naturally occurring neural computations during reward processing upon information about the connectivity of LH neurons. In addition, we used ex vivo patch-clamp experiments to explore the composition of GABAergic and glutamatergic LH inputs onto both DA and GABA neurons within the VTA. Building on our results from the recordings experiments, we utilized behavioral tasks to establish causal relationships between aspects of both reward seeking and feeding and the activation of distinct subsets of LH-VTA projections. Together, these data help us establish a model for how the components within the LH-VTA loop work together to process reward and how manipulating individual components can have profound effects on behavior.

RESULTS

Photoidentification of Distinct Components in the LH-VTA Circuit

In order to identify LH neurons that provide monosynaptic input to the VTA in vivo and observe their activity during freely moving behaviors, we used a dual-virus strategy to selectively express channelrhodopsin-2 (ChR2) in LH neurons providing monosynaptic input to the VTA (Figures 1A and S1). We injected an adeno-associated viral vector (AAV_5) carrying ChR2-eYFP in a Cre-recombinase-dependent double-inverted open reading frame (DIO) construct into the LH to infect local somata and injected a retrogradely traveling herpes simplex virus (HSV) carrying Cre-recombinase into the VTA. Subsequent recombination permitted opsin and fluorophore expression selectively in LH neurons providing monosynaptic input to the VTA. To confirm our approach, we performed ex vivo whole-cell patch-clamp recordings in horizontal brain slices containing the LH and recorded from neurons expressing ChR2-eYFP, as well as neighboring LH neurons that were ChR2-eYFP negative (Figure 1B). Light-evoked spike latencies, measured from light-pulse onset to the peak of the action potential, ranged from 3–8 ms (Figure 1C). We also found that none of the non-expressing (ChR2-negative) cells recorded showed excitatory responses to photostimulation (n = 14; Figure 1C), despite their proximity to ChR2-expressing cells.

In order to perform optogenetically mediated photoidentification in vivo, an optrode was implanted into the LH to record neuronal activity during a sucrose-seeking task. In the same recording session, we provided several patterns of photostimulation to identify ChR2-expressing LH-VTA neurons (Figures 1D and S1). We examined the distribution of excitatory photoresponse latencies across all LH neurons displaying a time-locked change in firing rate in response to illumination and observed a bimodal distribution (Figure 1E). We observed a population of neurons during in vivo recordings with latencies in a range of 3–8 ms. This was identical to the latency range found in ChR2-expressing LH-VTA neurons when we recorded ex vivo. We termed these units "Type 1" units (Figures 1C, 1E, and 1F). In addition, there was a distinct population of cells with ~100 ms photoresponse latencies (Figures 1E and 1G), and we termed these "Type 2" units. We also observed neurons that were inhibited in response to photostimulation of LH-VTA neurons (Figure S2), and we termed these "Type 3" units. We compared the action potential duration (as measured from peak to trough) and mean firing rates of Type 1 and Type 2 units as well as those that did not show a photoresponse (Figure 1H). The distribution of action potential durations of Type 1 (Figure 1I) and Type 2 (Figure 1J) units shows that the majority of Type 1 units have an action potential duration less than 500 μs (84%; n = 16/19, binomial distribution, p = 0.002).

Although Type 1 units fit standard criteria to be classified as ChR2 expressing (Cohen et al., 2012; Zhang et al., 2013), it was unclear whether the longer latency photoresponse of Type 2 units was indicative of ChR2-expressing neurons that responded more slowly to photostimulation, or whether this effect was due to network activity. Given that the ChR2-expressing (Type 1) LH neurons project directly to the VTA, one possibility was that Type 2 neurons were receiving feedback from the VTA (Figure 1K). Another possibility was that Type 2 neurons were activated by axon collaterals from Type 1 neurons (Figure 1L). To differentiate between these two possible circuit models, we inhibited the VTA in conjunction with photoidentification in the LH.

Long Latency Photoresponses in LH Neurons Are Mediated by Feedback from the VTA

Based on our circuit models, we would expect distal inhibition to have no effect on the photoresponses of ChR2-expressing LH neurons. However, if photoresponsive, but non-expressing, LH neurons relied on feedback from the VTA to elicit a time-locked response to illumination (Figure 1K), we would expect an attenuation of photoresponses in these neurons upon VTA inhibition. We expressed ChR2 in LH-VTA cells as above, but this time also expressed enhanced halorhodopsin 3.0 (NpHR) in the VTA and implanted an optic fiber in the VTA in addition to the optrode in LH (Figure 2A). We delivered the same blue-light illumination patterns in the LH for all three epochs but also photoinhibited the VTA with yellow light in the second epoch (Figure 2A).

The photoresponses of Type 1 units to blue-light illumination in the LH were unaffected by photoinhibition of the VTA, which is consistent with ChR2 expression in Type 1 LH-VTA neurons (Figure 2B). In contrast, the majority of Type 2 units (87%; n = 13/15, binomial distribution, p = 0.004) showed a significant attenuation of photoresponses to blue-light pulses delivered in the LH upon photoinhibition of VTA neurons. The responses of Type 1 and Type 2 units during VTA photoinhibition were significantly different (chi-square = 7.64, p = 0.0057; Figures 2B and 2C). These differences can also be seen in the max Z scores during individual epochs (Figure 2D) and with the yellow-ON epoch normalized to the yellow-OFF epoch (Figure 2E). These data suggest that Type 2 LH neurons receive input (either directly or indirectly) from the VTA (Figure 1K) rather than via local axon collaterals (Figure 1L).

Distinct Encoding Properties of LH Neurons Either upstream or downstream of the VTA

Having identified these two distinct types of LH neurons in the LH-VTA loop, we wanted to examine naturally occurring neural activity during a sucrose self-administration task (Figure 3A). Mice were trained to perform nosepoke responses for a cue predicting sucrose delivery at an adjacent port (as in Tye et al., 2008). To allow us to differentiate neural responses to the nosepoke and the cue, the cue and sucrose were delivered on a partial reinforcement schedule, wherein 50% of nosepokes were paired with a cue and sucrose delivery.

Type 1 units showed phasic responses to sucrose port entry, as seen in a representative Type 1 unit (Figure 3B), as well as the population data for all Type 1 units (Figure 3C). The phasic responses of Type 2 units, however, mainly reflected responses to the reward-predictive cue (Figures 3D and 3E). The normalized firing patterns of all recorded neurons (n = 198, divided into Type 1, 2, 3, and non-responsive units) are displayed for each task component: nosepokes paired with the cue, nosepokes in the absence of the cue, and sucrose port entry (Figure 3F). All Type 1 units that showed task-relevant phasic changes in activity

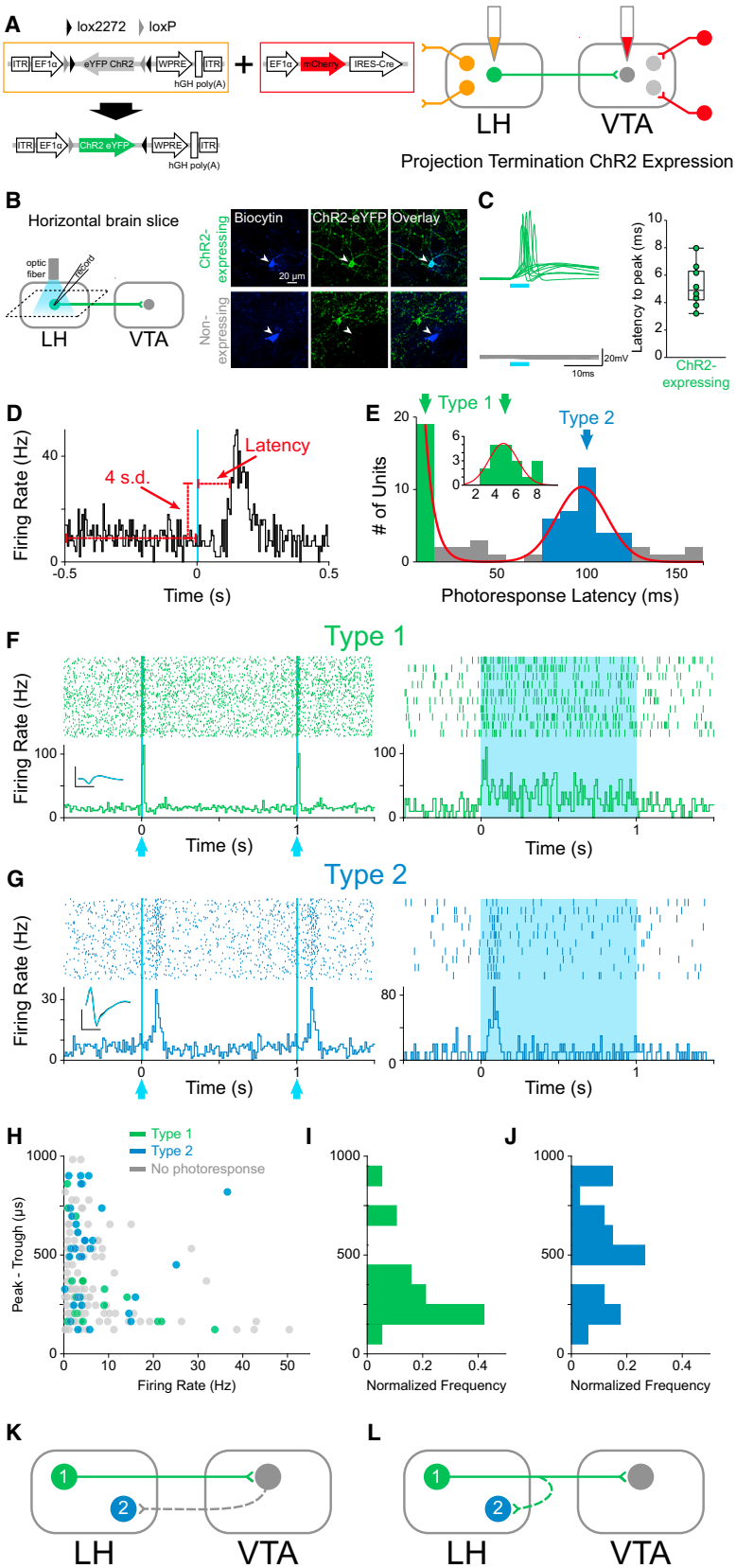

Figure 1. Phototagging LH-VTA Projections Reveals Two Populations of Neurons with Different Response Latencies to Photostimulation

(A) Wild-type mice (n = 12) were injected with AAV_5-DIO-ChR2-eYFP into the lateral hypothalamus (LH) and HSV-EF1α-IRES-Cre-mCherry into the ventral tegmental area (VTA).

(B) Horizontal brain slices containing the LH were prepared for whole-cell patch-clamp recordings in ChR2-expressing and non-expressing LH neurons.

(C) Individual traces recorded in current-clamp mode showing the response of ChR2-expressing (green, n = 10) and non-expressing (gray, n = 14) cells to a 5 ms pulse of 473 nm light are shown. The box and whisker plot shows the average response latency for each ChR2-expressing cell ex vivo.

(D) Photoresponse latencies in vivo were calculated by measuring the time from stimulation to 4 SD above the baseline firing rate.

(E) A bimodal distribution of excitatory photoresponse latencies was identified in recorded units (n = 198) and divided into Type 1 (green; n = 19) and Type 2 units (blue; n = 34).

(F) Type 1 units responded to photostimulation with fast excitation (3–8 ms latency). Inset shows the overlaid average traces for spontaneous spiking (black) and light-evoked spiking (blue) from a representative unit.

(G) Type 2 units responded to photostimulation with delayed excitation (80–120 ms latency).

(H) Scatterplot depicting the peak-trough duration of the waveform plotted against the average firing rate for each unit.

(I and J) Normalized histogram showing the distribution of peak-trough durations for Type 1 units (I) and Type 2 units (J).

(K and L) Diagrams illustrating two possible circuit models. (K) Type 1 units project directly from the LH to the VTA, whereas Type 2 units represent a population in the LH that is receiving feedback from the VTA; or (L) Type 2 units represent a population in the LH that is receiving input from collaterals of Type 1 units. Dotted lines indicate the presence of either a monosynaptic or polysynaptic connection.

Scale bar: y axis, 0.2 mV; x axis, 500 μs. See also Figure S1.

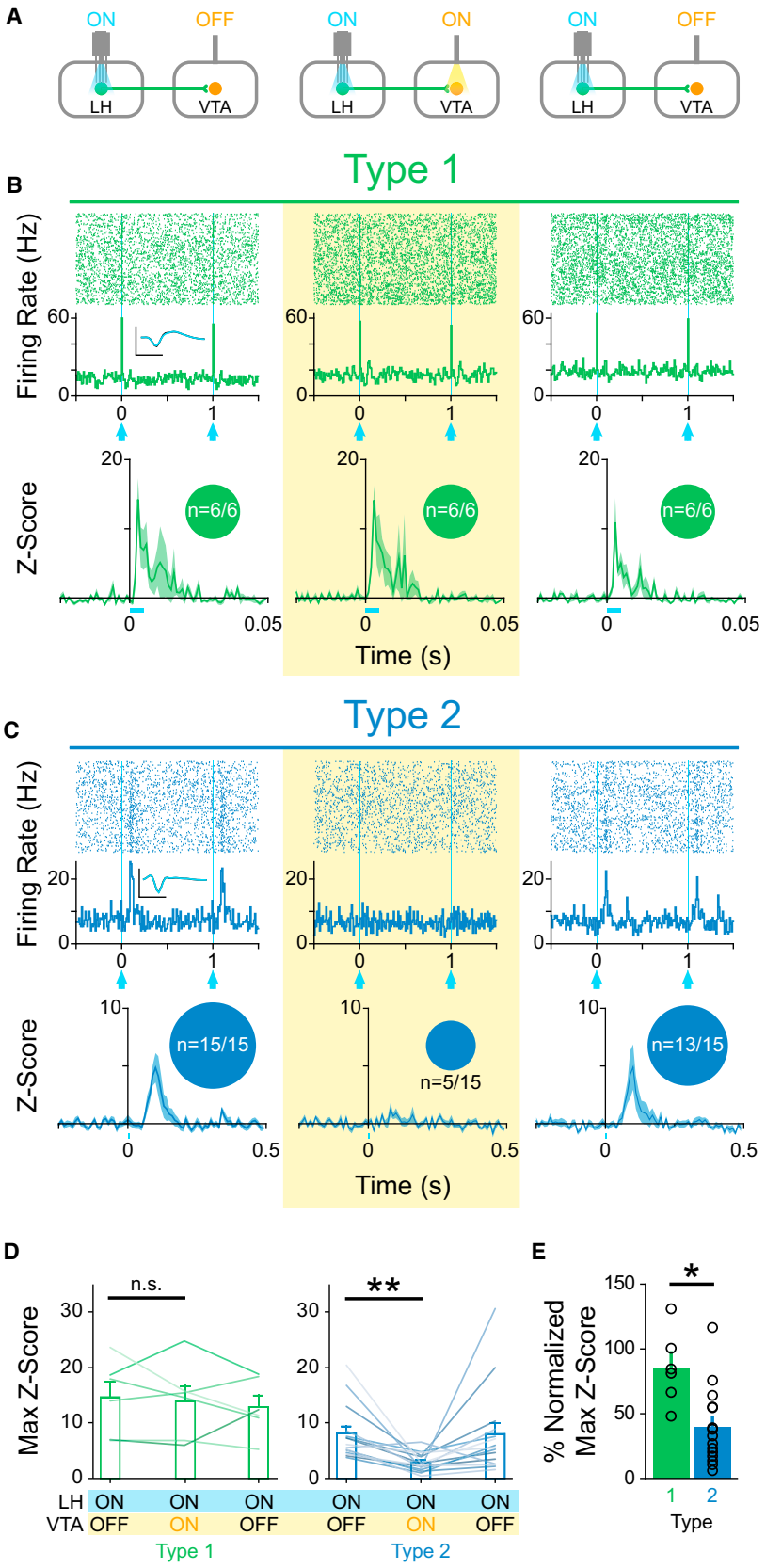

Figure 2. Inhibition of the VTA Selectively Attenuates the Photoresponse of Type 2, but not Type 1, Units

(A) Mice expressing ChR2 in LH-VTA projections received an additional injection of AAV_5-CaMKIIα-eNpHR3.0-eYFP into the VTA to allow for transient inhibition of VTA neurons by yellow light. Three epochs of phototagging were conducted (LH photoactivation: ON-ON-ON, VTA photoinhibition: OFF-ON-OFF).

(B) Type 1 (n = 6/121 units, n = 6 animals) photoresponse properties were unaffected (0%; n = 0/6 attenuated or abolished) by VTA inhibition. Inset circles represent the number of units photoresponsive during each epoch. Inset shows the overlaid average traces for spontaneous spiking (black) and light-evoked spiking (blue) from a representative unit.

(C) Type 2 (n = 15/121 units, n = 6 animals) photoresponse properties were abolished (67%; n = 10/15) or attenuated (87%; n = 13/15) during NpHR-mediated VTA inhibition.

(D) No significant difference in max Z score was detected between epochs with and without inhibition of the VTA for Type 1 units (two-tailed, paired Student's t test, p = 0.71). The max Z score was significantly lower in the ON (LH blue light illumination + VTA photoinhibition) epoch relative to the first OFF epoch (LH blue light illumination only) for Type 2 units (two-tailed, paired Student's t test, **p = 0.0015).

(E) There was a significant difference in max Z score (normalized to the OFF epoch) during photoinhibition of the VTA between Type 1 units compared to Type 2 units (two-tailed, unpaired Student's t test, *p = 0.014).

Error bars indicate + SEM. Scale bar: y axis, 0.2 mV; x axis, 500 μs. See also Figure S3.

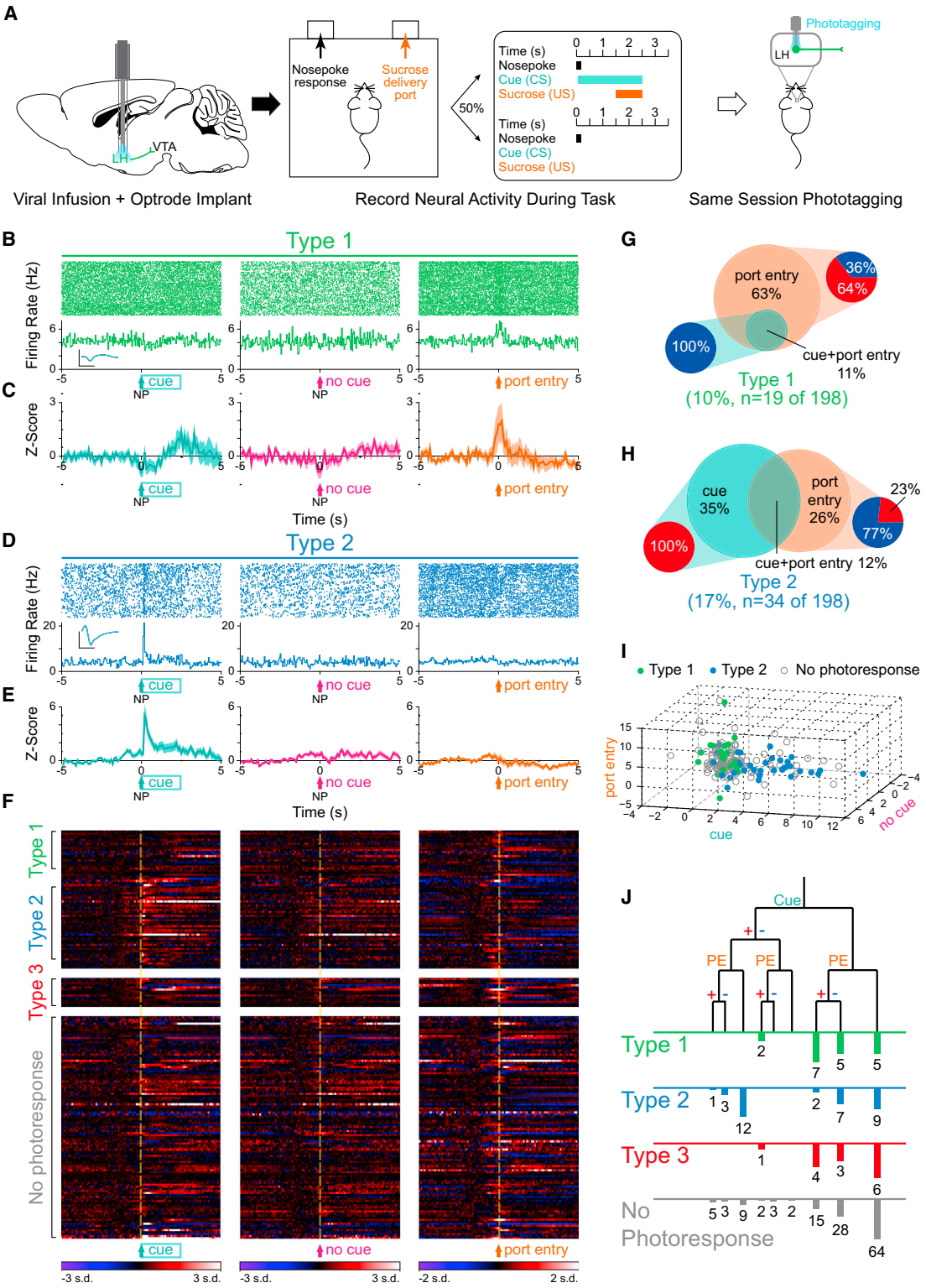

Figure 3. Type 1 Units Predominantly Respond to the Port Entry, whereas Type 2 Units Respond to Both the Conditioned Stimulus and the Port Entry

(A) Mice with optrodes implanted in the LH and expressing ChR2 in LH-VTA projections were trained on a task where 50% of nosepokes (NP) were followed by a cue (conditioned stimulus; CS) that predicts the delivery of sucrose (unconditioned stimulus; US) at the delivery port. In vivo electrophysiological recordings were performed during the behavioral task followed by phototagging in the same recording session to identify units by projection target.

(legend continued on next page)

(74%; n = 14/19) were either phasically excited or inhibited by sucrose port entry, with a small number also showing phasic inhibition to the reward-predictive cue (Figures 3B, 3C, and 3G). In contrast, Type 2 units were more heterogeneous, with task-responsive neurons encoding the cue selectively (35%), the sucrose port-entry selectively (26%), or both the cue and port entry (12%; Figures 3D, 3E, and 3H). To illustrate the strength of responses of Type 1 and Type 2 units to task-related events, we plotted each cell on a three-dimensional plot according to Z score (Figure 3I). To show the distribution of phasic changes in firing to multiple task-related events on a qualitative level, we plotted the number of cells of each photoresponse type that fell into a given category (Figure 3J).

Different Components of the LH-VTA Circuit Represent Distinct Aspects of Reward-Related Behavior

Given the well-defined role of the VTA in reward-prediction error (e.g., the phasic reduction of DA neuron firing in response to the unexpected omission of a reward and the phasic excitation in response to unexpected reward delivery) (Schultz et al., 1997), we investigated whether LH neurons would encode the unexpected omission of a sucrose reward. To do this, we recorded the neural activity of photoresponsive neurons during the same cue-reward task in well-trained animals but randomly omitted 30% of sucrose deliveries following the cue (Figure 4A).

The majority of Type 1 units (88%; n = 15/17, binomial distribution, p = 0.001) were insensitive to reward omission (Figures 4B and 4D), whereas a large subset of Type 2 units (67%; n = 12/18) showed a significantly different response to reward-presented and reward-omitted trials (Figures 4C and 4D). We concluded that LH-VTA (Type 1) neurons encoded the action of entering the port, as these port-entry responses were persistent even upon reward omission (Figure 4D), in contrast to Type 2 units (chi-square = 10.9804, p = 0.0009).

To determine whether Type 1 responses to port entry were truly encoding the conditioned response (CR), as opposed to general reward-seeking or exploratory behavior, we recorded in untrained mice that had not yet acquired the task. In task-naive mice, we delivered sucrose to the port in the absence of a predictive cue (unpredicted reward delivery) and found that Type 1 units did not show phasic responses to port entry (Figures 4E, 4F, and 4I), consistent with the model that Type 1 neurons encode the CR (Figure 4J).

Next, to determine whether Type 2 unit activity is consistent with a reward-prediction error-like response profile, we also recorded these neurons in well-trained animals during unpredicted reward delivery (Figure 4G). We found that a subset of Type 2 units responded to unpredicted sucrose deliveries (50%; Figures 4G–4I). Taken together, subsets of Type 2 units are sensitive to unexpected reward omission (Figures 4C and 4D) and unpredicted reward delivery (Figures 4G–4I), consistent with a reward-prediction error-like response profile.

Photostimulation of the LH-VTA Pathway Promotes Sucrose Seeking in the Face of a Negative Consequence

As we have shown above, Type 1 units represent a neural correlate of CR. Importantly, the increase in firing rate begins prior to CR, ramping up until the CR has been completed (Figures 3B, 3C, and 4B). To determine whether activation of the LH-VTA pathway could promote CR, we wanted to test the ability of LH-VTA activation in driving CR in the face of a negative consequence. In wild-type mice, we expressed ChR2-eYFP or eYFP alone in LH cell bodies and implanted an optic fiber over the VTA (Figures 5A and S4). Conversely, to test the role of the LH-VTA pathway in mediating CR or feeding-related behaviors, we bilaterally expressed NpHR-eYFP or eYFP alone in LH cells and implanted an optic fiber above the VTA (Figures 5A and S4).

We designed a Pavlovian conditioning task in which food-deprived mice had to cross a shock grid to retrieve a sucrose reward (Figure 5B). In the first "baseline" epoch (with the shock grid off), we verified that each mouse had acquired the Pavlovian conditioned approach task. In the second ("Shock") epoch, the shock grid delivered mild foot shocks every second. Finally, in the third epoch ("Shock+Light"), we continued to deliver foot shocks but also illuminated LH terminals in the VTA with blue light (10 Hz) in mice expressing ChR2 and matched eYFP controls and yellow light (constant) for mice expressing NpHR and their eYFP controls (Figure 5B).

We observed a significantly higher number of port entries per cue during the Shock+Light epoch and a significantly higher difference score (Shock+Light epoch − Shock-only epoch) in ChR2 mice relative to eYFP mice (Figure 5C and Movie S1). In contrast, photoinhibition of the LH-VTA pathway resulted in a significant

(B) Perievent raster histograms for a representative Type 1 unit that responded to port entry, but not to the reward-predictive cue. Inset shows overlaid average traces for spontaneous spiking (black) and light-evoked spiking (blue) from a representative unit.
(C) Population Z score plots showing the average responses of all Type 1 units (n = 19/198 units, n = 12 animals).
(D) Perievent raster histograms for a representative Type 2 unit that responded to the reward-predictive cue, but not to port entry.
(E) Population Z score plots show the average responses of all Type 2 units (n = 34/198 units, n = 12 animals).
(F) Heatmap representation of the individual Z scores of all units.
(G) Of all Type 1 units, 63% responded exclusively to the port entry (n = 12/19), whereas 11% responded to both the port entry and the reward-predictive cue (n = 2/19). Within the Type 1 units that responded to the port entry, 64% (n = 9/14) were excited (red) upon port entry, whereas 36% (n = 5/14) were inhibited (blue), and within the units that responded to the reward-predictive cue, 100% (n = 2/2) were inhibited by the cue.
(H) Of all Type 2 units, 35% (n = 12/34) responded exclusively to the reward-predictive cue, 26% (n = 9/34) responded exclusively to the port entry, and 12% (n = 4/34) responded to both. Within the Type 2 units that responded to the cue, 100% (n = 16/16) were excited by the cue, whereas none were inhibited, and within the units that responded to port entry, 77% (n = 10/13) were inhibited upon port entry, whereas 23% (n = 3/13) were excited.
(I) Graphical representation of Z scores during the experimental windows for cue, no cue, and port entry for Type 1, Type 2, and "no photoresponse" units.
(J) Diagram of recorded units demonstrating whether they responded to the cue or port entry (PE) and whether that response was with excitation (+) or inhibition (−).
Error bars indicate + SEM. Scale bar: y axis, 0.2 mV; x axis, 500 μs. See also Figure S2.

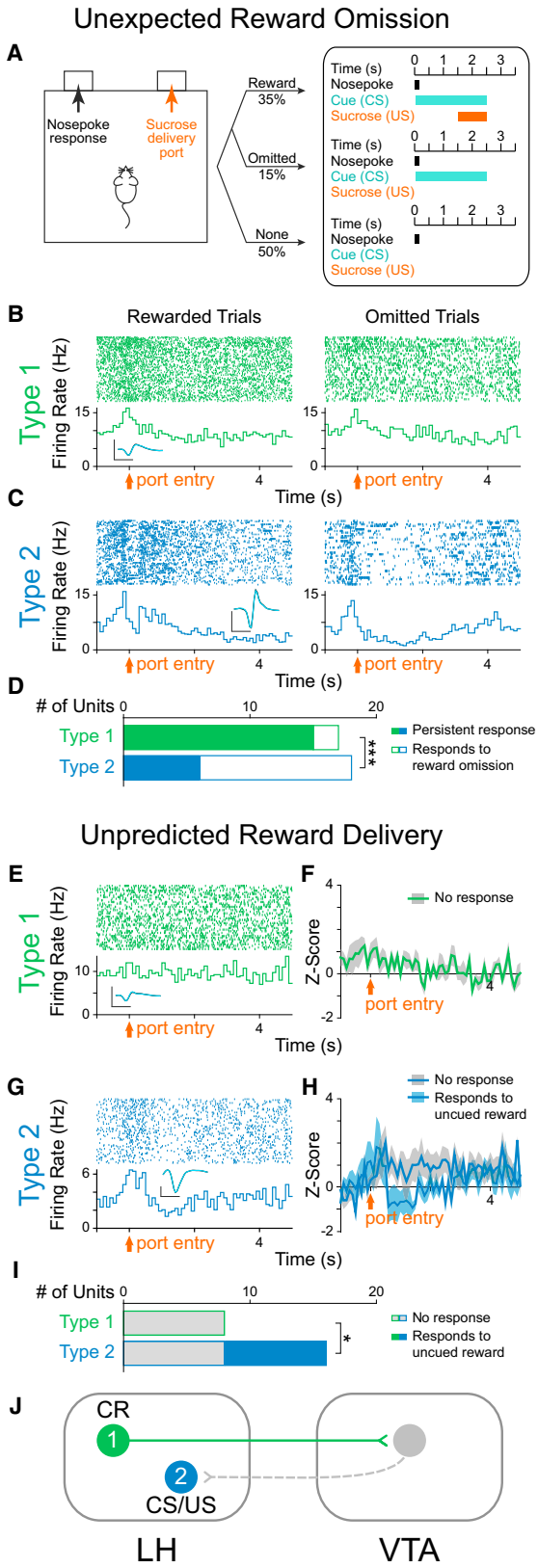

Figure 4. LH-VTA Neurons Encode the CR of Sucrose Seeking

(A) The original partial reinforcement sucrose self-administration task was modified so that in 30% of trials during which the reward-predictive cue was present, the expected sucrose delivery was omitted (15% of all trials).

(B) Perievent raster histograms of a Type 1 unit that showed no difference in response to port entry with reward omission. Inset shows overlaid average traces for spontaneous spiking (black) and light-evoked spiking (blue) from a representative unit.

(C) Perievent raster histograms of a Type 2 unit that showed a significantly different response to port entry upon omission of the expected reward.

(D) Of all Type 1 units recorded (n = 17/122 units, n = 6 animals), only 12% (n = 2/17) showed a significant difference in their responses when the expected reward was omitted. In contrast, of all Type 2 units recorded (n = 18/122 units, n = 6 animals), 67% (n = 12/18) showed a significant difference in their responses when the expected reward was omitted (chi-square = 10.9804, ***p = 0.0009).

(E) Unexpected sucrose delivery occurred in the absence of predictive cues. Perievent raster histogram of a Type 1 unit that did not respond to port entry following unpredicted reward delivery is shown.

(F) Population Z score plot showing the average responses of all Type 1 units to the port entry following unpredicted reward delivery.

(G) Perievent raster histogram of a Type 2 unit that showed an increase in firing rate to port entry following unpredicted reward delivery.

(H) Population Z score plot of Type 2 unit responses to port entry following unpredicted reward delivery, separated into those that showed a significant response and those that showed no significant response.

(I) Of all Type 1 units recorded (n = 8/105 units, n = 6 animals), 0% (n = 0/8) showed a significant response to the port entry following unpredicted reward delivery. In contrast, of all Type 2 units recorded (n = 16/105 units, n = 6 animals), 50% (n = 8/16) showed a significant response to the port entry following unpredicted reward delivery (chi-square = 6, *p = 0.0143).

(J) Schematic of the LH-VTA loop and the components of reward processing encoded by Type 1 and 2 cells. CR = conditioned response; CS = conditioned stimulus; US = unconditioned stimulus.

Scale bar: y axis, 0.2 mV; x axis, 500 μs.

reduction in port entries per cue and difference scores in the NpHR mice relative to eYFP mice (Figure 5D and Movie S2). Within-session extinction experiments during which cue presentations were not followed by sucrose deliveries showed similar trends in effect (Figure S4).

Importantly, we wanted to determine whether the changes in sucrose seeking we had obtained were caused by changes in feeding-related behavior or sensitivity to pain. We observed that photoactivation of the LH-VTA projection significantly increased the time spent feeding in well-fed mice in the ChR2 group (Figure 5E). However, photoinhibition of the LH-VTA pathway did not significantly reduce feeding (Figure 5F), even though these animals were food deprived to enhance our ability to detect a reduction relative to the baseline epoch (compare to sated animals in Figure 5E). In neither the ChR2 (Figure 5G) nor NpHR group (Figure 5H) did we observe a difference in latency to tail withdrawal from hot water (Ben-Bassat et al., 1959; Grotto and Sulman, 1967), indicating that manipulating the LH-VTA projection was not altering analgesia.

LH Provides Both Glutamatergic and GABAergic Input onto VTA DA and GABA Neurons

To study the composition of the fast transmission components of LH inputs to the VTA that were eliciting these effects, we performed whole-cell patch-clamp recordings from VTA neurons in an acute slice preparation while optically activating LH

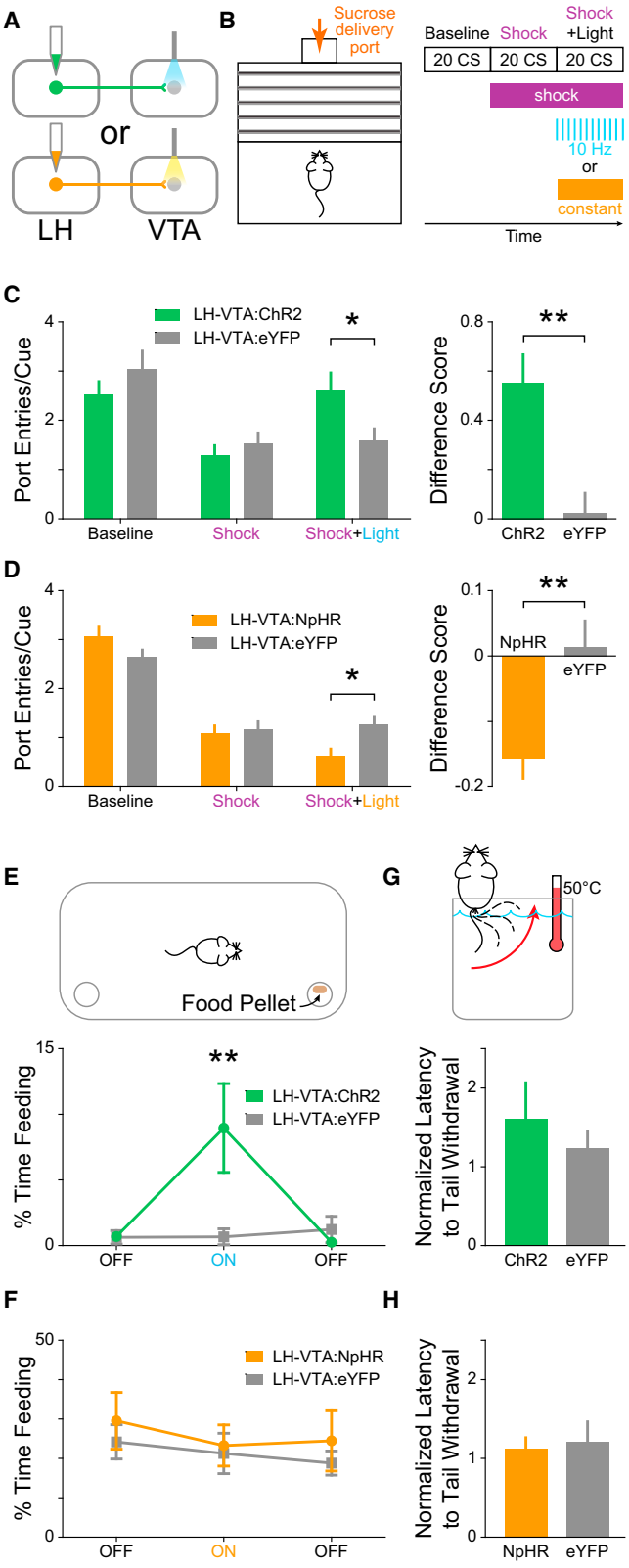

Figure 5. Excitation of LH-VTA Projections Promotes, whereas Inhibition Attenuates, Compulsive Sucrose Seeking

(A) Mice received injections of AAV_5-CaMKIIα-ChR2-eYFP (n = 8), AAV_5-CaMKIIα-eNpHR3.0-eYFP (n = 14), or AAV_5-CaMKIIα-eYFP (n = 6 controls for ChR2, n = 8 controls for NpHR) into the LH, and an optic fiber was implanted above the VTA.

(B) Mice were trained on a Pavlovian conditioned approach task wherein a cue predicted sucrose delivery to a port located across a shock grid. On test day, mice were presented with 20 cues during a baseline period without shock, 20 cues when the shock grid was on, and 20 cues during which 10 Hz blue or constant yellow light was delivered while the shock floor remained on.

(C) Mice in the ChR2 group showed a significant increase in the number of port entries per cue during the "Shock+Light" epoch relative to eYFP controls (n = 8 ChR2, n = 6 eYFP; two-way ANOVA revealed a group x epoch interaction, $F_{2,24} = 20.47$, $p < 0.0001$; Bonferroni post-hoc analysis, *$p < 0.05$). The difference between the number of port entries per cue during the "Shock+Light" epoch and "Shock" epoch was also significantly different between the ChR2 and eYFP control groups (two-tailed, unpaired Student's t test, **p = 0.0090).

(D) Mice in the NpHR group showed a significant decrease in the number of port entries per cue during the Shock+Light epoch relative to eYFP controls (n = 13 NpHR, n = 8 eYFP; two-way ANOVA revealed a group x epoch interaction, $F_{2,38} = 116.63$, $p < 0.0001$; Bonferroni post-hoc analysis, *$p < 0.05$). The difference score was also significantly different between the NpHR-expressing and eYFP control mice (two-tailed, unpaired Student's t test, **p = 0.0062).

(E) Mice were placed into an open chamber with two cups, one containing food and the other without, and behavior in three experimental epochs was recorded (light OFF-ON-OFF). ChR2-expressing mice showed a significant increase in feeding (measured by time spent consuming food) compared with eYFP controls during the epoch paired with blue-light stimulation (n = 8 ChR2, n = 6 eYFP; two-way ANOVA revealed a group x epoch interaction, $F_{2,24} = 4.23$, $p = 0.0268$; Bonferroni post-hoc analysis, **$p < 0.01$).

(F) NpHR-expressing mice showed no significant differences from eYFP control mice in time spent feeding in any of the epochs (n = 9 NpHR, n = 7 eYFP).

(G and H) To examine the effect of light stimulation on analgesia, mice had their tails placed into a heated water bath, and the latency-to-tail withdrawal was measured during two counterbalanced epochs (light ON-OFF). (G) ChR2-expressing mice showed no significant difference in tail-withdrawal latency (normalized to OFF epoch) during blue-light stimulation compared to eYFP controls (n = 8 ChR2, n = 6 eYFP), (H) nor did NpHR-expressing mice during yellow-light stimulation (n = 5 NpHR, n = 8 eYFP).

Error bars indicate ± SEM. See also Figure S4.

inputs expressing ChR2-eYFP (Figures 6A and S5). Given that there is well-established heterogeneity within the VTA, including ~65% DA neurons, ~30% GABA neurons, and ~5% glutamate neurons (Margolis et al., 2006; Nair-Roberts et al., 2008; Yamaguchi et al., 2007), we filled cells with biocytin while recording to allow for identification of cell type using post-hoc immunohistochemistry for tyrosine hydroxylase (TH; Figure 6B), in addition to recording the hyperpolarization-activated cation current (I_h) and mapping cell location (Figures 6B and S5).

First, we recorded in current-clamp during photostimulation of ChR2-expressing LH inputs and observed that 23 of 27 neurons showed a time-locked response to photostimulation of LH inputs (Figure 6C). The majority of DA neurons sampled in the VTA received a net excitatory input from the LH (56%), whereas another subset showed net inhibition (30%; Figure 6C). The spatial distribution of these DA neurons is mapped onto an atlas for horizontal slices containing the VTA (Figure 6D).

To establish the monosynaptic contribution of LH inputs to VTA DA neurons, we used ChR2-assisted circuit mapping, where voltage-clamp recordings were performed in the presence of tetrodotoxin (TTX) and 4-aminopyridine (4AP; Petreanu

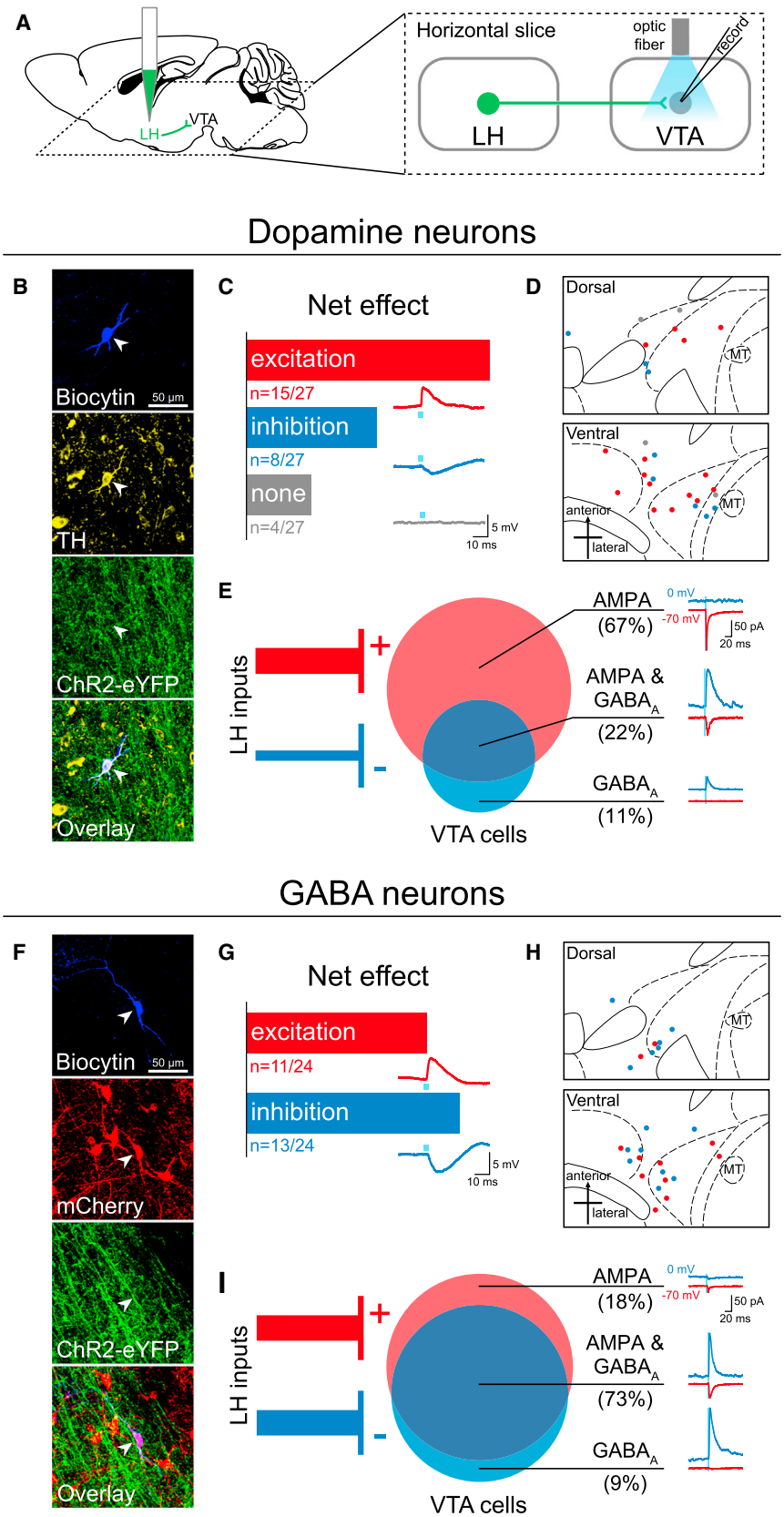

Figure 6. The LH Sends a Mixture of Excitatory and Inhibitory Projections to Both DA and GABA Neurons in the VTA

(A) AAV$_5$-CaMKIIα-ChR2-eYFP was injected into the LH, and at least 6 weeks later, 300 µm-thick horizontal brain slices were prepared containing the VTA. Whole-cell patch-clamp recordings were made in VTA neurons, and ChR2-expressing LH terminals were activated by illumination with 473 nm light via an optic fiber resting on the brain slice.

(B) Neurons were filled with biocytin during recording, and DA neurons were identified by immunohistochemistry for TH (n = 27).

(C) The net effect of optical stimulation of LH terminals was assessed in current-clamp mode, which revealed that 55% of DA neurons (n = 15/27) showed a net excitatory response, whereas 30% (n = 8/27) responded with net inhibition, and 15% (n = 4/27) showed no response. An example of an excitatory postsynaptic potential (EPSP, red trace), an inhibitory postsynaptic potential (IPSP, blue trace), and a non-responsive cell (gray trace) are shown below each bar.

(D) The distribution of all recorded TH$^+$ neurons plotted on horizontal midbrain slices with colors indicating the response to LH terminal photostimulation.

(E) VTA DA neurons received only AMPAR-mediated input (67%, n = 6/9), only GABA$_A$R-mediated input (11%, n = 1/9), or both of these currents (22%, n = 2/9).

(F) VTA GABA neurons were identified by the presence of mCherry (n = 24), achieved by injection of Cre-dependent AAV$_5$-EF1α-DIO-mCherry into the VTA of VGAT::Cre mice.

(G) Optical stimulation of LH terminals in current-clamp mode showed that GABA neurons respond with either net excitation (46%, n = 11/24) or net inhibition (54%, n = 13/24) to LH input.

(H) The distribution of each recorded GABA neuron plotted on horizontal midbrain slices with colors indicating the response to LH terminal stimulation.

(I) GABA neurons received a mixture of AMPAR-mediated and GABA$_A$R-mediated input from the LH (AMPA only: 18%, n = 2/11; AMPA & GABA$_A$: 73%, n = 8/11; GABA$_A$: 9%, n = 1/11).

MT = medial terminal nucleus of the accessory optic tract. See also Figures S5 and S6.

et al., 2007). Consistent with our observations from current-clamp recordings, we observed that the majority of recorded VTA DA neurons exclusively received excitatory monosynaptic input from the LH (67%), compared to VTA DA neurons that exclusively received inhibitory monosynaptic input (11%), or both (22%; Figures 6E and S6).

We identified VTA GABA neurons by injecting a Cre-dependent fluorophore (AAV_5-DIO-mCherry) into the VTA of VGAT::Cre mice and utilized mCherry expression to direct the recording of VTA GABA neurons (n = 24; Figure 6F). Forty-six percent of VTA GABA neurons responded with net excitation, whereas 54% responded with net inhibition, to photostimulation of ChR2-expressing LH inputs (Figure 6G). The spatial distribution of these cells is shown in Figure 6H. Upon examination of the monosynaptic input from the LH (as described above), we found that 18% of sampled GABA neurons received exclusively excitatory input and 9% received exclusively inhibitory input (Figure 6I). However, relative to VTA DA neurons, we found that more VTA GABA neurons received both excitatory AMPAR-mediated and inhibitory $GABA_AR$-mediated monosynaptic input from the LH (73%; chi-square = 5.0505, p = 0.0246; Figures 6I and S6).

Distinct Roles of Glutamatergic and GABAergic Components of the LH-VTA Pathway in Behavior

Given that our ex vivo recordings provided evidence supporting robust input from both GABAergic and glutamatergic LH projections to the VTA, we next probed the role of each component independently. To do this, we used transgenic mouse lines expressing Cre-recombinase in neurons that expressed either vesicular glutamate transporter 2 (VGLUT2) or vesicular GABA transporter (VGAT). We injected AAV_5-DIO-ChR2-eYFP or AAV_5-DIO-eYFP into the LH of VGLUT2::Cre and VGAT::Cre mice and implanted an optic fiber over the VTA (Figure S7). These animals were then run on each of the behavioral assays shown in Figure 5.

We did not observe any detectable differences in the number of port entries made per cue between mice expressing ChR2 or eYFP in the LH^{glut}-VTA projection (Figure 7A) or in the LH^{GABA}-VTA projection (Figure 7B). However upon video analysis, we noticed aberrant gnawing behaviors in the LH^{GABA}-VTA:ChR2 group upon blue-light illumination (see Movies S3 and S4). In LH^{glut}-VTA mice, although there was a trend toward a reduction in feeding upon photostimulation in the ChR2 group compared to the eYFP group, this was not statistically significant (Figure 7C). In contrast, we observed a robust increase in the time spent feeding in sated mice upon illumination in the LH^{GABA}-VTA:ChR2 group relative to controls (Figure 7D and Movie S3). In neither group of animals was there an effect of light stimulation in the tail-withdrawal assay (Figures 7E and 7F).

During the feeding task, as we did during the sucrose-seeking task, we again noticed aberrant feeding-related motor sequences that were not directed at food. We filmed a representative mouse in the LH^{GABA}-VTA:ChR2 group in an empty transparent chamber, and upon 20 Hz photostimulation, we observed unusual appetitive motor sequences such as licking and gnawing the floor or empty space (Movie S4). We quantified these "gnawing" behaviors during the feeding task in the wild-type LH-VTA (Figure 7G), LH^{glut}-VTA (Figure 7H), and LH^{GABA}-VTA (Figure 7I) groups and showed that LH^{GABA}-VTA:ChR2 mice gnawed more than wild-type or LH^{glut}-VTA:ChR2 mice when photostimulated, as compared to their respective eYFP groups (Figure 7J). We considered whether the aberrant feeding-related behaviors might be separated from appropriately directed feeding at lower frequencies. However, when we tested the LH^{GABA}-VTA:ChR2 group with 5 Hz and 10 Hz trains of blue light, we observed a proportional relationship between stimulation frequency and both feeding and gnawing (Figure 7K).

DISCUSSION

Functional Components of the LH-VTA Loop

The LH projection to the VTA has been explored with electrical stimulation collision studies (Bielajew and Shizgal, 1986) and has long been hypothesized to play a role in reward processing (Hoebel and Teitelbaum, 1962; Margules and Olds, 1962), yet pinpointing this role has been a challenge. Here, we are providing a detailed dissection of how individual components of the LH-VTA loop process different aspects of a reward-related task.

Through the use of optogenetic-mediated phototagging (Figure 1), we have identified two separate populations of LH neurons: cells that send projections to the VTA (Type 1) and cells that receive feedback from the VTA (Type 2; Figure 2)—though these populations need not be mutually exclusive, as it is possible that LH neurons could both send and receive inputs to and from the VTA. Interestingly, we found that relatively few photoresponsive neurons fell outside the bimodal distribution encapsulating these two populations (Figures S2B and 1E). Given this, in combination with the long latency delay in Type 2 photoresponses (~100 ms), we speculate that there may be one dominant pathway contributing to the activity of Type 2 neurons. Additionally, because DA binds G protein-coupled receptors, the kinetics are slower than most glutamatergic synapses (Girault and Greengard, 2004) and may explain this cluster of 100 ms latency photoresponsive units. It is also possible that the VTA may provide indirect feedback through other distal regions, via excitatory intermediate regions such as the amygdala, or with disinhibition via the nucleus accumbens (NAc) or bed nucleus of the stria terminalis (BNST).

Interestingly, whereas photostimulation of Type 1 units evokes excitatory responses in Type 2 units, Type 1 and 2 units show distinct behavioral encoding properties. For example, the numbers of Type 1 and Type 2 units that selectively encode the reward-predictive cue are significantly different (n = 0/19 Type 1 versus n = 12/34 Type 2, chi-square = 8.67, p = 0.003). This paradoxical response pattern could be due to computational processes at an intermediate circuit element, such as the VTA, that may be playing an active role during the behavioral task but inactive during phototagging. Additionally, the behavioral state of the animal could influence how these data are processed.

Decoding Circuit Components in Reward Processing

Our reward omission experiments allowed us to distinguish between LH neural encoding of the CR and the consumption of

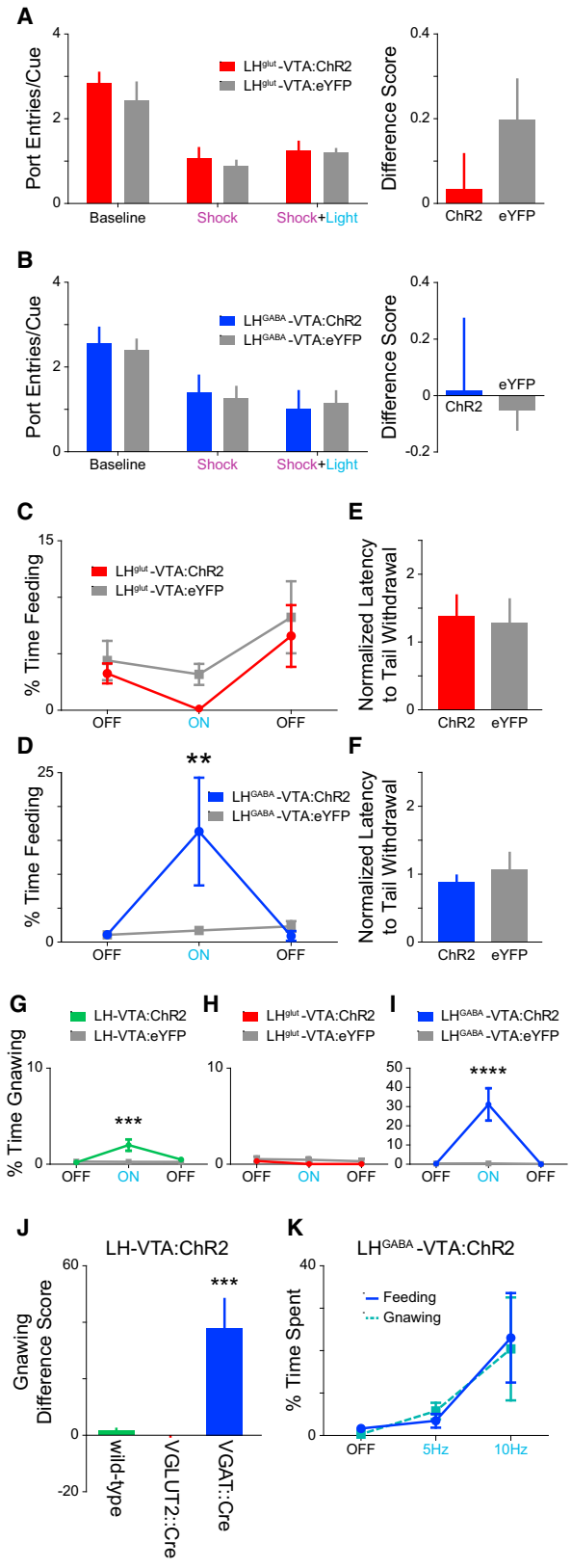

Figure 7. Photoactivation of the GABAergic, but Not the Glutamatergic, Component of the LH-VTA Projection Increased Feeding Behaviors

(A and B) In order to selectively activate glutamatergic or GABAergic LH-VTA projections, VGLUT2::Cre and VGAT::Cre mice received an injection of AAV_5-DIO-ChR2-eYFP or AAV_5-DIO-eYFP into the LH and had an optic fiber implanted over the VTA. In the sucrose-seeking task, there were no significant differences in the numbers of port entries per cue in any epoch for LH^{glut}-VTA:ChR2 mice (n = 7) compared to LH^{glut}-VTA:eYFP control mice (n = 6) (A) nor in those of LH^{GABA}-VTA:ChR2 mice (n = 6) compared to LH^{GABA}-VTA:eYFP mice (n = 8) (B).

(C) There was no significant difference between LH^{glut}-VTA:ChR2 mice and eYFP controls in feeding behavior.

(D) However, LH^{GABA}-VTA:ChR2 mice showed a significant increase in time spent feeding during light stimulation compared to LH^{GABA}-VTA:eYFP controls (two-way ANOVA revealed a group x epoch interaction, $F_{2,24} = 4.78$, $p = 0.0178$; Bonferroni post-hoc analysis, $^{**}p < 0.01$).

(E and F) Neither LH^{glut}-VTA:ChR2 mice (E) nor LH^{GABA}-VTA:ChR2 mice (F) showed a difference in tail withdrawal latency compared to their respective controls.

(G) LH-VTA:ChR2 mice showed a significant increase in time spent gnawing during the light ON epoch compared to eYFP controls (two-way ANOVA revealed a group x epoch interaction, $F_{2,24} = 4.78$, $p = 0.0179$; Bonferroni post-hoc analysis, $^{***}p < 0.001$).

(H) There was no significant difference between LH^{glut}-VTA:ChR2 and LH^{glut}-VTA:eYFP controls in gnawing behavior.

(I) However, LH^{GABA}-VTA:ChR2 animals also showed a significant increase in time spent gnawing during the light ON epoch compared to LH^{GABA}-VTA:eYFP controls (two-way ANOVA revealed a group x epoch interaction, $F_{2,24} = 18.91$, $p < 0.0001$; Bonferroni post-hoc analysis, $^{****}p < 0.0001$).

(J) The difference score for gnawing behavior between the ON and OFF epochs was significantly greater in LH^{GABA}-VTA:ChR2 animals in comparison with either wild-type LH-VTA:ChR2 or LH^{glut}-VTA:ChR2 animals (one-way ANOVA, $F_{2,18} = 16.76$, $p < 0.0001$; Bonferroni post-hoc analysis, $^{***}p < 0.001$).

(K) Frequency-response curve showing the effect of different blue-light stimulation frequencies (OFF, 5 Hz, 10 Hz) on behavior in LH^{GABA}-VTA:ChR2 animals.

Error bars indicate ± SEM. See also Figure S7.

the unconditioned stimulus (US). In these experiments, a subset of Type 2 units responded to the reward-predictive cue (CS) and the US and also showed a decrease in firing rate when expected rewards were omitted. Furthermore, a subset of Type 2 units also show phasic excitation upon unexpected reward delivery (Figures 4G and 4H). These data are reminiscent of the way DA neurons in the VTA encode reward-prediction error (Cohen et al., 2012; Schultz et al., 1997). We speculate that VTA neurons may transmit reward-prediction error signals to a subset of LH neurons, which are well-positioned to integrate these signals for the determination of an appropriate behavioral output. Specifically, the LH is robustly interconnected with a multitude of other brain areas (Berthoud and Münzberg, 2011) and has been causally linked to homeostatic states such as sleep/arousal and hunger/satiety (Carter et al., 2009; Jennings et al., 2013).

A Causal Role for the LH-VTA Pathway in Compulsive Sucrose Seeking?

Compulsive reward-seeking behavior has primarily been discussed in the context of drug addiction, wherein a classic paradigm for compulsive drug seeking has been to examine the degree to which drug-seeking behavior persists in the face of a negative consequence, such as a foot shock (Belin et al., 2008; Pelloux et al., 2007; Vanderschuren and Everitt, 2004). We

adapted this task for sucrose seeking to allow us to investigate whether activation of the LH-VTA pathway was sufficient to promote compulsive sucrose seeking. Given that a distinct difference between drug and natural reward is that drug rewards are not necessary for survival, there is controversy as to what behaviors would constitute compulsive sucrose- or food-seeking behavior. An alternative interpretation of our data is that activation of the LH-VTA pathway simply increases motivational drive or the urge to seek appetitive reinforcers. As the rates of obesity have increased in recent decades (Mietus-Snyder and Lustig, 2008), compulsive overeating and sugar addiction are prevalent conditions that are a major threat to human health (Avena, 2007). The feeding behavior in sated (fully fed) mice after activation of the LH-VTA pathway is reminiscent of eating behaviors seen in humans diagnosed with compulsive overeating disorder (or binge-eating disorder) (DSM-V).

It has been proposed that repeated actions lead to the formation of habits, which themselves lead to the compulsive reward seeking that characterizes addiction (Everitt and Robbins, 2005). Our finding that LH-VTA neurons only encode port entry after conditioning suggests that this pathway is selectively encoding a conditioned response, not just a motivated action. This is consistent with our observations that optically activating this projection can promote compulsive reward seeking in the face of a negative consequence (Figure 5C), as well as in the absence of need (as seen in sated mice, Figure 5E). This interpretation is further substantiated by our finding that photoinhibition of the LH-VTA pathway selectively reduces compulsive sucrose seeking (Figure 5D) but does not reduce feeding in food-restricted mice (Figure 5F). One of the greatest challenges in treating compulsive overeating or binge-eating disorders is the risk of impairing feeding behaviors in general. From a translational perspective, we may have identified a specific neural circuit as a potential target for the development of therapeutic interventions for compulsive overeating or sugar addiction without sacrificing natural feeding behaviors.

Composition of LH Input to the VTA

We show that in addition to a glutamatergic LH-VTA component (Kempadoo et al., 2013), there is also a significant GABAergic component in the projection (Leinninger et al., 2009), and that LH neurons synapse directly onto both DA and GABA neurons in the VTA (Figure 6). However, there is a difference in the balance of the excitatory/inhibitory input onto VTA DA and GABA neurons.

While we used immunohistochemical processing to verify the identity of VTA neurons, we also measured I_h, a hyperpolarization-activated inwardly rectifying non-specific cation current (Lacey et al., 1989; Ungless and Grace, 2012). The presence of this current has been widely used in electrophysiological studies to identify DA neurons, but it has been shown to be present only in subpopulations of DA neurons, delineated by projection target (Lammel et al., 2011). Although it has previously been proposed in a review by Fields and colleagues that "LH neurons synapse onto VTA projections to the PFC, but not those projecting to the NAc" (Fields et al., 2007), our data suggest that this controversy be reopened for further investigation. Even though we did observe a subset of DA neurons that received net excitation from the LH and possessed a very small I_h (consistent with mPFC- or NAc medial shell-projecting DA neurons), we also observed a subset of DA neurons that received net excitatory input and showed a large I_h (consistent with characteristics of DA neurons projecting to the lateral shell of the NAc; Figure S5; Lammel et al., 2011). Conversely, VTA DA neurons that received a net inhibitory input showed a very small I_h or lacked this current, which is consistent with the notion that the LH sends predominantly inhibitory input onto VTA DA neurons projecting to the mPFC or the medial shell of the NAc. We also show that LH inputs can be observed in both medial and lateral VTA, suggesting that the LH provides inputs onto VTA neurons with diverse projection targets, as it is known that VTA projection target corresponds somewhat to spatial location along a medial-lateral axis (Lammel et al., 2008).

Excitation/Inhibition Balance in the LH-VTA Pathway

The role of the LH-VTA pathway in promoting reward has previously been ascribed to glutamatergic transmission in the VTA (Kempadoo et al., 2013), as the CaMKIIα promoter is often thought to be selective for excitatory projection neurons. However, our data clearly show that expressing ChR2 under the control of the CaMKIIα promoter also targets GABAergic projection neurons in the LH (Figure 6).

The behavior elicited by photostimulation of the LH^{GABA}-VTA pathway was frenzied, mis-directed, and maladaptive (Movie S4). One interpretation is that activation of the LH^{GABA}-VTA pathway sends a signal to the mouse that causes the recognition of an appetitive reinforcer. An alternative interpretation is that the LH^{GABA}-VTA pathway might drive incentive salience or an intense "wanting," consistent with a signal underlying conditioned approach, but at a non-physiological level that produces this aberrant feeding-related behavior (Berridge and Robinson, 2003). Consistent with this, it is possible that activation of the LH^{GABA}-VTA projection actually produces intense sensations of craving, or urges to feed. However, our experiments show that activation of LH^{GABA}-VTA does not produce an increase in compulsive sucrose seeking, but this is likely due to the excessive gnawing and aberrant appetitive behaviors focused on non-food objects in the testing chamber. Although it is difficult to determine the experience of the mouse during this manipulation, it is clear that appropriately directed feeding-related behaviors require the coordinated activation of both the GABAergic and glutamatergic components of the LH-VTA pathway.

Conclusion

Optogenetic and pharmacogenetic manipulations are powerful tools for establishing causal relationships, yet they do not reveal the endogenous, physiological properties of neural circuit elements. Our study unifies information about the synaptic connectivity, the naturally occurring endogenous function, and the causal role of the LH-VTA pathway, providing a new level of insight toward how information is integrated in this circuit. These results highlight the importance of examining the functional role of neurons by connectivity, in addition to genetic markers. LH-VTA neurons selectively encoded the action of reward seeking

but did not encode environmental stimuli, whereas rewarding stimuli and reward-predictive cues were encoded by a discrete population of LH neurons downstream of the VTA. Furthermore, we have identified a specific projection that is causally linked to compulsive sucrose-seeking and feeding behavior. The heterogeneity in the LH-VTA projection is necessary for providing an adaptive balance between driving motivation and regulating appropriately directed appetitive behaviors. These findings provide insights relevant to pathological conditions such as compulsive overeating disorder, sugar addiction, and obesity.

EXPERIMENTAL PROCEDURES

Phototagging VTA-Projecting LH Neurons

To limit expression of ChR2 to only LH neurons projecting to the VTA, AAV_5-DIO-ChR2-eYFP was injected into the LH and HSV-EF1α-IRES-Cre-mCherry into the VTA. In NpHR inhibition experiments, AAV_5-CaMKIIα-eNpHR3.0-eYFP was injected into the VTA as well. An optrode was implanted in the LH and an optic fiber over the VTA.

Partial Reinforcement Sucrose Retrieval Task

For in vivo recording, animals were trained on a partial reinforcement sucrose retrieval task, where 50% of nosepokes were followed by a cue predicting the delivery of sucrose at the port entry. Adjustments were made to this task to examine the effects on reward omission by omitting sucrose deliveries from a subset of cues and to examine the effects on unexpected reward by the delivery of sucrose without the existence of the cue.

Sucrose Seeking in the Face of a Negative Consequence

To study the effect on conditioned responding by stimulation of LH-VTA projections, we developed a task wherein an animal must cross a shock floor to obtain a sucrose reward. Wild-type animals with ChR2, NpHR, or eYFP injected either unilaterally (AAV_5-CaMKIIα-ChR2-eYFP) or bilaterally (AAV_5-CaMKIIα-eNpHR3.0-eYFP) in the LH with an optic fiber placed over VTA or VGLUT2::Cre and VGAT::Cre animals with AAV_5-DIO-ChR2-eYFP injection in the LH and optic fiber over the VTA were tested. Because LH-VTA:ChR2 mice showed an increase in sucrose seeking in the face of a negative consequence, these animals were sated before evaluating the effects of photostimulation on feeding on normal chow. In contrast, LH-VTA:NpHR mice showed a decrease in sucrose seeking in the face of a negative consequence and were therefore mildly food restricted before testing the effects of photostimulation on feeding on normal chow.

Ex Vivo Characterization of LH-VTA

Whole-cell patch-clamp recordings were used to study the input of LH neurons onto DA and GABA VTA neurons. DA neurons were identified by filling cells with biocytin and post-hoc immunostaining for TH. GABA cells were identified during recordings by fluorescence due to AAV_5-DIO-mCherry injection into the VTA of VGAT::Cre animals.

SUPPLEMENTAL INFORMATION

Supplemental Information includes Extended Discussion, Extended Experimental Procedures, seven figures, and four movies and can be found with this article online at http://dx.doi.org/10.1016/j.cell.2015.01.003.

AUTHOR CONTRIBUTIONS

E.H.N. and G.A.M. performed electrophysiological recordings and analyses for in vivo and ex vivo experiments, respectively. S.A.A., E.H.N., K.N.P., and C.A.L. performed behavioral experiments. R.W., K.N.P., C.A.L., and E.H.N. performed histological verification. R.N. provided HSV virus. K.M.T. and C.P.W. supervised experiments and trained experimentalists. E.H.N., G.A.M., S.A.A., and K.M.T. designed experiments. E.H.N. and K.M.T. wrote the manuscript; all authors contributed to the editing and revision of manuscript.

ACKNOWLEDGMENTS

We thank N. Golan, R. Thomas, M. Anahtar, G. Glober, and A. Beyeler for their assistance with immunohistochemistry. We would also like to thank C. Seo, and S. Kim for their contributions throughout the project and M. Wilson and P. Shizgal for helpful discussion. K.M.T. is a New York Stem Cell Foundation - Robertson Investigator and acknowledges funding from the JPB Foundation, PIIF, PNDRF, Whitehall Foundation, Klingenstein Foundation, NARSAD Young Investigator Award, Alfred P. Sloan Foundation, Whitehead Career Development Chair, NIH R01-MH102441-01 (NIMH), and NIH Director's New Investigator Award DP2-DK-102256-01 (NIDDK). E.H.N. was supported by the NSF Graduate Research Fellowship, the Integrative Neuronal Systems Fellowship, and the Training Program in the Neurobiology of Learning and Memory. G.A.M. was supported by the Simons Center for the Social Brain Postdoctoral Fellowship. S.A.A. was supported by the Jeffrey and Nancy Halis Fellowship as well as the Henry E. Singleton Fund. C.A.L. was supported by the Integrative Neuronal Systems Fellowship and the James R. Killian Fellowship. R.W. was supported by the Netherlands Organisation for Scientific Research (NWO) RUBICON fellowship program.

Received: July 22, 2014
Revised: November 2, 2014
Accepted: December 23, 2014
Published: January 29, 2015

REFERENCES

Avena, N.M.; Experimental and Clinical Psychopharmacology (2007). Examining the addictive-like properties of binge eating using an animal model of sugar dependence. Exp. Clin. Psychopharmacol. *15*, 481–491.

Barone, F.C., Wayner, M.J., Scharoun, S.L., Guevara-Aguilar, R., and Aguilar-Baturoni, H.U. (1981). Afferent connections to the lateral hypothalamus: a horseradish peroxidase study in the rat. Brain Res. Bull. *7*, 75–88.

Beckstead, R.M., Domesick, V.B., and Nauta, W.J. (1979). Efferent connections of the substantia nigra and ventral tegmental area in the rat. Brain Res. *175*, 191–217.

Belin, D., Mar, A.C., Dalley, J.W., Robbins, T.W., and Everitt, B.J. (2008). High impulsivity predicts the switch to compulsive cocaine-taking. Science *320*, 1352–1355.

Ben-Bassat, J., Peretz, E., and Sulman, F.G. (1959). Analgesimetry and ranking of analgesic drugs by the receptacle method. Arch. Int. Pharmacodyn. Ther. *122*, 434–447.

Berridge, K.C., and Robinson, T.E. (2003). Parsing reward. Trends Neurosci. *26*, 507–513.

Berthoud, H.-R., and Münzberg, H. (2011). The lateral hypothalamus as integrator of metabolic and environmental needs: from electrical self-stimulation to opto-genetics. Physiol. Behav. *104*, 29–39.

Bielajew, C., and Shizgal, P. (1986). Evidence implicating descending fibers in self-stimulation of the medial forebrain bundle. J. Neurosci. *6*, 919–929.

Burton, M.J., Rolls, E.T., and Mora, F. (1976). Effects of hunger on the responses of neurons in the lateral hypothalamus to the sight and taste of food. Exp. Neurol. *51*, 668–677.

Carter, M.E., Adamantidis, A., Ohtsu, H., Deisseroth, K., and de Lecea, L. (2009). Sleep homeostasis modulates hypocretin-mediated sleep-to-wake transitions. J. Neurosci. *29*, 10939–10949.

Cohen, J.Y., Haesler, S., Vong, L., Lowell, B.B., and Uchida, N. (2012). Neuron-type-specific signals for reward and punishment in the ventral tegmental area. Nature *482*, 85–88.

Everitt, B.J., and Robbins, T.W. (2005). Neural systems of reinforcement for drug addiction: from actions to habits to compulsion. Nat. Neurosci. *8*, 1481–1489.

Fields, H.L., Hjelmstad, G.O., Margolis, E.B., and Nicola, S.M. (2007). Ventral tegmental area neurons in learned appetitive behavior and positive reinforcement. Annu. Rev. Neurosci. *30*, 289–316.

Girault, J.A., and Greengard, P. (2004). The neurobiology of dopamine signaling. Arch. Neurol. *61*, 641–644.

Gratton, A., and Wise, R.A. (1988). Comparisons of refractory periods for medial forebrain bundle fibers subserving stimulation-induced feeding and brain stimulation reward: a psychophysical study. Brain Res. *438*, 256–263.

Grotto, M., and Sulman, F.G. (1967). Modified receptacle method for animal analgesimetry. Arch. Int. Pharmacodyn. Ther. *165*, 152–159.

Hoebel, B.G., and Teitelbaum, P. (1962). Hypothalamic control of feeding and self-stimulation. Science *135*, 375–377.

Jennings, J.H., Rizzi, G., Stamatakis, A.M., Ung, R.L., and Stuber, G.D. (2013). The inhibitory circuit architecture of the lateral hypothalamus orchestrates feeding. Science *341*, 1517–1521.

Kempadoo, K.A., Tourino, C., Cho, S.L., Magnani, F., Leinninger, G.-M., Stuber, G.D., Zhang, F., Myers, M.G., Deisseroth, K., de Lecea, L., and Bonci, A. (2013). Hypothalamic neurotensin projections promote reward by enhancing glutamate transmission in the VTA. J. Neurosci. *33*, 7618–7626.

Lacey, M.G., Mercuri, N.B., and North, R.A. (1989). Two cell types in rat substantia nigra zona compacta distinguished by membrane properties and the actions of dopamine and opioids. J. Neurosci. *9*, 1233–1241.

Lammel, S., Hetzel, A., Häckel, O., Jones, I., Liss, B., and Roeper, J. (2008). Unique properties of mesoprefrontal neurons within a dual mesocorticolimbic dopamine system. Neuron *57*, 760–773.

Lammel, S., Ion, D.I., Roeper, J., and Malenka, R.C. (2011). Projection-specific modulation of dopamine neuron synapses by aversive and rewarding stimuli. Neuron *70*, 855–862.

Leinninger, G.M., Jo, Y.-H., Leshan, R.L., Louis, G.W., Yang, H., Barrera, J.G., Wilson, H., Opland, D.M., Faouzi, M.A., Gong, Y., et al. (2009). Leptin acts via leptin receptor-expressing lateral hypothalamic neurons to modulate the mesolimbic dopamine system and suppress feeding. Cell Metab. *10*, 89–98.

Margolis, E.B., Lock, H., Hjelmstad, G.O., and Fields, H.L. (2006). The ventral tegmental area revisited: is there an electrophysiological marker for dopaminergic neurons? J. Physiol. *577*, 907–924.

Margules, D.L., and Olds, J. (1962). Identical "feeding" and "rewarding" systems in the lateral hypothalamus of rats. Science *135*, 374–375.

Mietus-Snyder, M.L., and Lustig, R.H. (2008). Childhood obesity: adrift in the "limbic triangle". Annu. Rev. Med. *59*, 147–162.

Nair-Roberts, R.G., Chatelain-Badie, S.D., Benson, E., White-Cooper, H., Bolam, J.P., and Ungless, M.A. (2008). Stereological estimates of dopaminergic, GABAergic and glutamatergic neurons in the ventral tegmental area, substantia nigra and retrorubral field in the rat. Neuroscience *152*, 1024–1031.

Nakamura, K., Ono, T., and Tamura, R. (1987). Central sites involved in lateral hypothalamus conditioned neural responses to acoustic cues in the rat. J. Neurophysiol. *58*, 1123–1148.

Norgren, R. (1970). Gustatory responses in the hypothalamus. Brain Res. *21*, 63–77.

Olds, J., and Milner, P. (1954). Positive reinforcement produced by electrical stimulation of septal area and other regions of rat brain. J. Comp. Physiol. Psychol. *47*, 419–427.

Paxinos, G., and Franklin, K.B.J. (2001). The Mouse Brain in Stereotaxic Coordinates, Second Edition (New York: Academic Press).

Pelloux, Y., Everitt, B.J., and Dickinson, A. (2007). Compulsive drug seeking by rats under punishment: effects of drug taking history. Psychopharmacology (Berl.) *194*, 127–137.

Petreanu, L., Huber, D., Sobczyk, A., and Svoboda, K. (2007). Channelrhodopsin-2-assisted circuit mapping of long-range callosal projections. Nat. Neurosci. *10*, 663–668.

Petreanu, L., Mao, T., Sternson, S.M., and Svoboda, K. (2009). The subcellular organization of neocortical excitatory connections. Nature *457*, 1142–1145.

Schultz, W., Dayan, P., and Montague, P.R. (1997). A neural substrate of prediction and reward. Science *275*, 1593–1599.

Schwartzbaum, J.S. (1988). Electrophysiology of taste, feeding and reward in lateral hypothalamus of rabbit. Physiol. Behav. *44*, 507–526.

Simon, H., Le Moal, M., and Calas, A. (1979). Efferents and afferents of the ventral tegmental-A10 region studied after local injection of [3H]leucine and horseradish peroxidase. Brain Res. *178*, 17–40.

Singh, J., Desiraju, T., and Raju, T.R. (1996). Comparison of intracranial self-stimulation evoked from lateral hypothalamus and ventral tegmentum: analysis based on stimulation parameters and behavioural response characteristics. Brain Res. Bull. *41*, 399–408.

Tabuchi, E., Yokawa, T., Mallick, H., Inubushi, T., Kondoh, T., Ono, T., and Torii, K. (2002). Spatio-temporal dynamics of brain activated regions during drinking behavior in rats. Brain Res. *951*, 270–279.

Tye, K.M., Stuber, G.D., de Ridder, B., Bonci, A., and Janak, P.H. (2008). Rapid strengthening of thalamo-amygdala synapses mediates cue-reward learning. Nature *453*, 1253–1257.

Ungless, M.A., and Grace, A.A. (2012). Are you or aren't you? Challenges associated with physiologically identifying dopamine neurons. Trends Neurosci. *35*, 422–430.

Vanderschuren, L.J.M.J., and Everitt, B.J. (2004). Drug seeking becomes compulsive after prolonged cocaine self-administration. Science *305*, 1017–1019.

Watabe-Uchida, M., Zhu, L., Ogawa, S.K., Vamanrao, A., and Uchida, N. (2012). Whole-brain mapping of direct inputs to midbrain dopamine neurons. Neuron *74*, 858–873.

Wise, R.A. (2004). Dopamine, learning and motivation. Nat. Rev. Neurosci. *5*, 483–494.

Yamaguchi, T., Sheen, W., and Morales, M. (2007). Glutamatergic neurons are present in the rat ventral tegmental area. Eur. J. Neurosci. *25*, 106–118.

Yamamoto, T., Matsuo, R., Kiyomitsu, Y., and Kitamura, R. (1989). Response properties of lateral hypothalamic neurons during ingestive behavior with special reference to licking of various taste solutions. Brain Res. *481*, 286–297.

Zhang, S.-J., Ye, J., Miao, C., Tsao, A., Cerniauskas, I., Ledergerber, D., Moser, M.-B., and Moser, E.I. (2013). Optogenetic dissection of entorhinal-hippocampal functional connectivity. Science *340*, 1232627.